Supplementary Information

Supplementary methods

Preparation and inoculation of anaerobic ACS medium

To prepare dinitrogen gas (N_2)-sparged ACS medium, we boiled the medium for 10 minutes and then cooled it to room temperature while under a constant stream of dinitrogen gas. After reaching room temperature, we decanted 20 ml of the medium into 25-ml serum bottles and sealed the serum bottles with gas-tight stoppers, leaving a headspace of approximately 5 ml of dinitrogen gas. We inoculated the dinitrogen gas-sparged ACS medium with overnight cultures of *P. stutzeri* strains using aseptic syringes. We used a pH electrode to verify that the pH of the culture medium remained unchanged over the time-course of the experiments.

Chemical analysis of nitrate and nitrite concentrations

We thawed and diluted cell-free liquid samples into deionized water at a dilution of 1:100 (vol:vol). We constructed standard curves for nitrate (NO_3^-) and nitrite (NO_2^-) by dissolving the required mass into aerobic ACS medium (0, 2, 4, 6, 8 and 10 mM for each) and then diluting the standards into deionized water at a dilution of 1:100 (vol:vol). We analyzed the standards and samples for nitrate and nitrite using the Metrohm 930 Compact IC Flex system and the Metrohm 887 Professional UV/Vis Detector. We used the Metrohm 889 IC Sample Center, the Metrohm Metrosep A Supp 16; 5x4 mm guard column, the Metrohm Metrosep A Supp 16; 250x4 mm analytical column with a column temperature of 45°C, an eluent consisting of 7.5 mM Na_2CO_3/0.75 mM NaOH and a flow rate of 0.8 ml/min.

Biosensor experiments to measure nitrate and nitrite directly during denitrification

We used NO_x^- and NO_2^- biosensors from Unisense (Aarhus, Denmark) to measure nitrate and nitrite concentrations during denitrification. The biosensors consist of an electrochemical N_2O transducer and a biochamber which contains bacteria that reduce both NO_3^- and NO_2^- (NO_x^- sensor) or only NO_2^- (NO_2^- sensor) to N_2O, which is then detected by this electrochemical transducers. Thus, by using both sensors, real-time concentrations of nitrate and nitrite are measured. We picked a single colony of the completely-consuming strain (strain A1601), let it grow overnight in aerobic ACS media, and then inoculated 1 ml of this aerobic culture into a 2L batch of aerobic ACS medium amended with 2 mM of sodium nitrate ($NaNO_2$). The cultures contained no headspace, thus preventing oxygen from entering the medium. Once the culture had reached stationary-phase, we amended the cultures with 200 µM of nitrate or nitrite sequentially. The biosensors were first calibrated by measuring nitrate and nitrite additions to a salt solution with the same pH and temperature as the bacterial culture. The biosensors were attached to a microsensor multimeter that was connected to a computer loaded with the Unisense software and measurements were logged every 0.5 seconds.

Gene deletion methods

We deleted the *narG*, *nirS*, and *comA* genes from *P. stutzeri* 1501 using derivatives of the *sacB*-containing conditionally replicative pAW19 plasmid (Metcalf *et al*., 1996; White and Metcalf, 2004). The derivative plasmids contain deletions in the *narG*, *nirS*, or *comA* genes and are designated pAW19-*ΔnarG*, pAW19-*ΔnirS*, and pAW19-*ΔcomA*, respectively. To construct these derivative plasmids, we first introduced pAW19 into *Escherichia coli* DH5α/λpir (Miller and Mekalanos, 1988) via electroporation and purified pAW19 from an

overnight culture. We next amplified 1 kbp regions immediately upstream and downstream of the translational start and stop sites of the *narG*, *nirS*, and *comA* genes using *Taq* DNA polymerase and the amplification primers listed in Supplementary Table 1. These amplification primers contain the *Spe*I, *Not*I, and *Sac*I sites that we used to clone the amplification products into pAW19. We then digested the PCR amplification products and pAW19 with the appropriate restriction enzymes and sequentially ligated the upstream and downstream amplification products into pAW19. Finally, we introduced each of the assembled derivative plasmids into *E. coli* BW20767 (Metcalf *et al*., 1996) via electroporation.

We delivered the pAW19-*ΔnarG*, pAW19-*ΔnirS*, or pAW19-*ΔcomA* plasmid into *P. stutzeri* A1501 by conjugative mating with *E. coli* BW20767 as the plasmid donor (Metcalf *et al*., 1996). We selected *P. stutzeri* exconjugants by plating on MOPS agar plates containing 0.2% citrate and 50 μg ml^{-1} of kanamycin (White and Metcalf; 2004). We selected *P. stutzeri* plasmid segregant mutants by plating on TYE agar plates containing 5% sucrose (Metcalf *et al*., 1996). We verified plasmid segregation by testing for kanamycin sensitivity on LB agar plates containing 50 μg ml^{-1} of kanamycin. We identified deletion segregant mutants by analyzing the size of PCR products generated with the forward amplification primer for the upstream 1 kbp region and the reverse amplification primer for the downstream 1 kbp region (Supplementary Table 1).

Phenotype validation

We experimentally verified that the *narG* and *nirS* deletions caused the desired phenotypes by testing whether the *P. stutzeri* mutant strains could grow in dinitrogen gas-sparged ACS

liquid medium amended with 10 mM of sodium nitrate ($NaNO_3$) or sodium nitrite ($NaNO_2$). The Δ*nirS* mutant strain (strain A1603) grew in medium amended with 10 mM of nitrate but did not grow in medium amended with 10 mM of nitrite. Conversely, the Δ*narG* mutant strain (strain A1602) did not grow in medium amended with 10 mM of nitrate but grew in medium amended with 10 mM of nitrite. Mixtures of the Δ*nirS* and Δ*narG* mutant strains (strains A1602 and A1603) could grow together in medium amended with 10 mM of nitrate but no nitrite, thus confirming the establishment of a nitrite cross-feeding co-culture. We further used PCR amplification to verify that the correct deletions are present in each strain.

Mathematical model

We used the NDsolve function of Mathematica software (version 8.0.1.0) and the kinetic parameters reported by Bryan *et al*. (1985) and Almeida *et al*. (1995a, 1995b) to predict the kinetics of cell growth, nitrate (NO_3^-) consumption, and nitrite (NO_2^-) production and consumption. We predicted the kinetics for a completely consuming strain using Equations 1 to 5, where $X_{complete}$ is the biomass concentration of the completely consuming strain [g L^{-1}], Y_i is the yield coefficient for biomass production [g $mmol^{-1}$], v_i is the specific substrate consumption rate [mmol g^{-1} min^{-1}], $S_{i,in}$ is the substrate concentration within the periplasm of the cell [mM], $S_{i,out}$ is the substrate concentration of the bulk medium [mM], K_{perm} is the permeability coefficient for mass transfer between the periplasm and the bulk medium [min^{-1} V_{cell}^{-1}], and V_{cell} is the volume of cells per g cells.

$$\frac{dX_{complete}}{dt} = Y_{NO_3^-} \cdot v_{NO_3^-} + Y_{NO_2^-} \cdot v_{NO_2^-} \quad (1)$$

$$\frac{dS_{NO_3^-,in}}{dt} \cdot V_{cell} = -v_{NO_3^-} + K_{perm} \cdot \left(S_{NO_3^-,out} - S_{NO_3^-,in}\right) \quad (2)$$

$$\frac{dS_{NO_2^-,in}}{dt} \cdot V_{cell} = v_{NO_3^-} - v_{NO_2^-} + K_{perm} \cdot \left(S_{NO_2^-,out} - S_{NO_2^-,in}\right) \quad (3)$$

$$\frac{dS_{NO_3^-,out}}{dt} = -X_{complete} \cdot K_{perm} \cdot \left(S_{NO_3^-,out} - S_{NO_3^-,in}\right) \quad (4)$$

$$\frac{dS_{NO_2^-,out}}{dt} = -X_{complete} \cdot K_{perm} \cdot \left(S_{NO_2^-,out} - S_{NO_2^-,in}\right) \quad (5)$$

We calculated the specific substrate consumption rates using the following two equations, where v_{max_i} is the maximum substrate consumption rate [mmol g^{-1} min^{-1}], K_{m_i} is the Michaelis-Menton coefficient for substrate limitation [mM], and $K_{I_{NO_2^-}}$ is the inhibition coefficient for nitrite [mM].

$$v_{NO_3^-} = \frac{v_{max_{NO_3^-}} \cdot S_{NO_3^-,in}}{K_{m_{NO_3^-}} + S_{NO_3^-,in} + \left(\frac{S_{NO_2^-,in}{}^2}{K_{I_{NO_2^-}}}\right)} \quad (6)$$

$$v_{NO_2^-} = \frac{\left(v_{max_{NO_2^-}} - \left(\frac{v_{NO_3^-} \cdot v_{max_{NO_2^-}}}{v_{max_{NO_3^-}}}\right)\right) \cdot S_{NO_2^-,in}}{K_{m_{NO_2^-}} + S_{NO_2^-,in} + \left(\frac{S_{NO_2^-,in}{}^2}{K_{I_{NO_2^-}}}\right)} \quad (7)$$

There are three notable features of this system of equations. First, we explicitly accounted for mass transfer across the cell. Second, the term $-\left(\frac{v_{NO_3^-} \cdot v_{max_{NO_2^-}}}{v_{max_{NO_3^-}}}\right)$ in the numerator of Equation 7 accounts for competition between the nitrate and nitrite reductases for reduced electron carriers as described by Almeida *et al*. (1995b). The consequence of this term is that the rate of nitrate consumption represses the rate of nitrite consumption. Third, the term $\left(\frac{S_{NO_2^-,in}{}^2}{K_{I_{NO_2^-}}}\right)$ in Equations 6 and 7 is the Andrews inhibition term and accounts for the pH-dependent inhibitory effects of nitrite as proposed by Wang *et al.* (1995).

For the nitrite (NO_2^-) cross-feeding strains, we predicted the kinetics of cell growth, nitrate (NO_3^-) consumption, and nitrite production and consumption using Equations 8 to 15, where X_{prod} is the biomass concentration of the nitrite producing strain [g L^{-1}], X_{cons} is the biomass concentration of the nitrite consuming strain [g L^{-1}], $S_{i,in,prod}$ is the substrate concentration within the periplasm of the nitrite producing strain [mM], $S_{i,in,cons}$ is the substrate concentration within the periplasm of the nitrite consuming strain [mM], and all other parameters are identical to those described for Equations 1 to 5.

$$\frac{dX_{prod}}{dt} = Y_{NO_3^-} \cdot v_{NO_3^-} \quad (8)$$

$$\frac{dX_{cons}}{dt} = Y_{NO_2^-} \cdot v_{NO_2^-} \quad (9)$$

$$\frac{dS_{NO_3^-,in,prod}}{dt} \cdot V_{cell} = -v_{NO_3^-} + K_{perm} \cdot \left(S_{NO_3^-,out} - S_{NO_3^-,in,prod}\right) \quad (10)$$

$$\frac{dS_{NO_3^-,in,cons}}{dt} \cdot V_{cell} = K_{perm} \cdot \left(S_{NO_3^-,out} - S_{NO_3^-,in,cons}\right) \quad (11)$$

$$\frac{dS_{NO_2^-,in,prod}}{dt} \cdot V_{cell} = v_{NO_3^-} + K_{perm} \cdot \left(S_{NO_2^-,out} - S_{NO_2^-,in,prod}\right) \quad (12)$$

$$\frac{dS_{NO_2^-,in,cons}}{dt} \cdot V_{cell} = -v_{NO_2^-} + K_{perm} \cdot \left(S_{NO_2^-,out} - S_{NO_2^-,in,cons}\right) \quad (13)$$

$$\frac{dS_{NO_3^-,out}}{dt} = -X_{prod} \cdot K_{perm} \cdot \left(S_{NO_3^-,out} - S_{NO_3^-,in,prod}\right) - X_{cons} \cdot K_{perm} \cdot \left(S_{NO_3^-,out} - S_{NO_3^-,in,cons}\right) \quad (14)$$

$$\frac{dS_{NO_2^-,out}}{dt} = -X_{prod} \cdot K_{perm} \cdot \left(S_{NO_2^-,out} - S_{NO_2^-,in,prod}\right) - X_{cons} \cdot K_{perm} \cdot \left(S_{NO_2^-,out} - S_{NO_2^-,in,cons}\right) \quad (15)$$

We calculated the specific substrate consumption rates using the following two equations, where v_{max_i} is the maximum substrate consumption rate [mmol g^{-1} min^{-1}], K_{m_i} is the Michaelis-Menton coefficient for substrate limitation [mM], and $K_{I_{NO_2^-}}$ is the inhibition coefficient for nitrite [mM].

$$v_{NO_3^-} = \frac{v_{max_{NO_3^-}} \cdot S_{NO_3^-,in,prod}}{K_{m_{NO_3^-}} + S_{NO_3^-,in,prod} + \left(\frac{S_{NO_2^-,in,prod}{}^2}{K_{I_{NO_2^-}}}\right)} \quad (16)$$

$$v_{NO_2^-} = \frac{v_{max_{NO_2^-}} \cdot S_{NO_2^-,in,cons}}{K_{m_{NO_2^-}} + S_{NO_2^-,in,cons} + \left(\frac{S_{NO_2^-,in,cons}{}^2}{K_{I_{NO_2^-}}}\right)} \quad (17)$$

The main difference between this system of equations and the system of equations for the completely denitrifying cell-type is that the competition term $-\left(\frac{v_{NO_3^-} \cdot v_{max_{NO_2^-}}}{v_{max_{NO_3^-}}}\right)$ in the numerator of Equation 7 is absent from Equation 17. This is because the nitrate and nitrite reductases are segregated into different cells and, consequently, the specific and maximum nitrate consumption rates are zero.

In summary, the main assumptions of the model are i) substrate consumption and growth kinetics can be simulated using Micheli-Menton kinetics, ii) the rate of nitrate consumption directly represses the rate of nitrite consumption when the nitrate and nitrite reductases are contained within the same cell, and ii) inter-enzyme competition is eliminated when the nitrate and nitrite reductases are segregated into different cells.

Supplementary results

Independent repetition of the effect of pH on growth

We repeated the test of whether differences in pH itself cause differences in the maximum specific growth rate (u_{max} [min^{-1}]) of completely-consuming cells (strain A1601). We set the pH of the culture medium to 7.5 or 6.5 and grew completely-consuming cells under aerobic conditions. We measured the zero-order maximum specific growth rate (u_{max}) from ten consecutive data points that coincide with the most rapid period of growth. The data are plotted in Supplementary Figure 2. We found that reducing the pH from 7.5 to 6.5 had no observable negative effect on the maximum specific growth rate (two-sample Welch test, two-sided $P > 0.8$, n = 8).

pH-dependence of nitrite inhibition in the absence of oxygen

We tested whether nitrite (NO_2^-) causes pH-dependent growth inhibition in the absence of oxygen. We set the pH of the culture medium to 7.5 or 6.5 and grew completely-consuming cells (strain A1601) under anaerobic conditions. After 72 hours of incubation, cells inoculated into medium at pH 7.5 with 10 mM of exogenous nitrite had reached stationary phase. In contrast, cells inoculated into medium at pH 6.5 with 10 mM of exogenous nitrite had no observable growth. Thus, nitrite has pH-dependent effects on growth under anaerobic conditions.

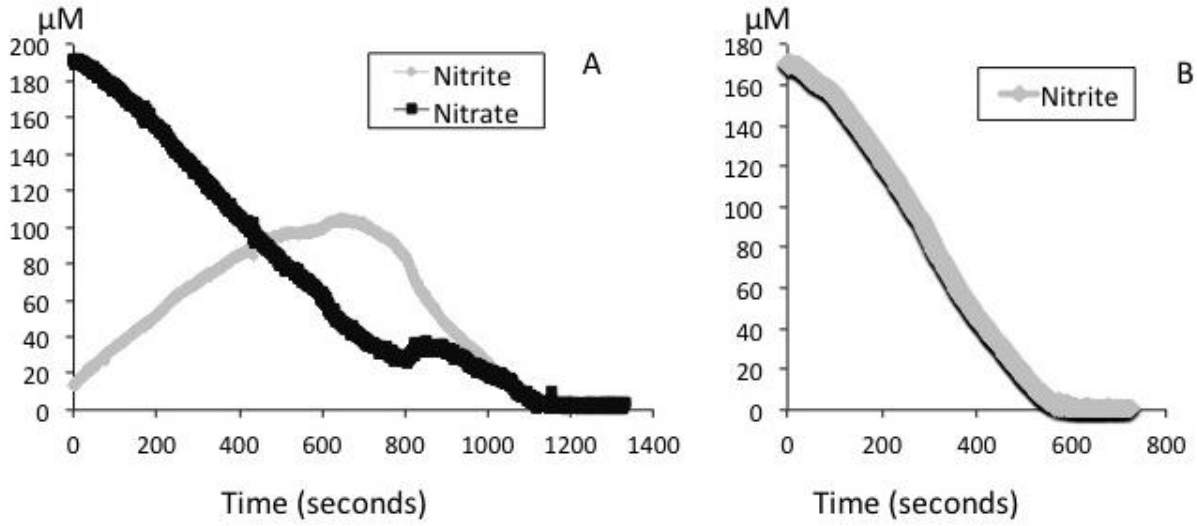

Supplementary Figure 1 Nitrate and nitrite consumption dynamics. We amended anaerobic stationary-phase cultures with 200 µM of (**a**) nitrate (NO_3^-) or (**b**) nitrite (NO_2^-) and measured nitrate and nitrite concentrations with biosensors over time. The consumption of nitrate and nitrite began immediately without an apparent lag.

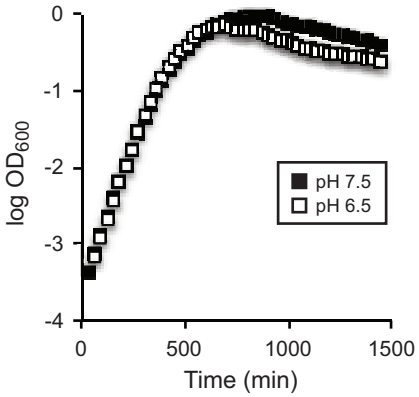

Supplementary Figure 2 Repeated measurements of the effect of pH on growth. We grew completely-consuming cells (strain A1601) at pH 7.5 (black squares) or pH 6.5 (white squares) under aerobic conditions and in the absence of nitrite (NO_2^-) and measured the OD_{600} values over time. We only plotted every fourth data point to facilitate visualization. Data points are the average measurements among eight independent biological replicates for each pH. The zero-order maximum growth rates are not significantly different from each other (two-sample Welch test, two-sided $P > 0.8$, $n_1 = n_2 = 8$).

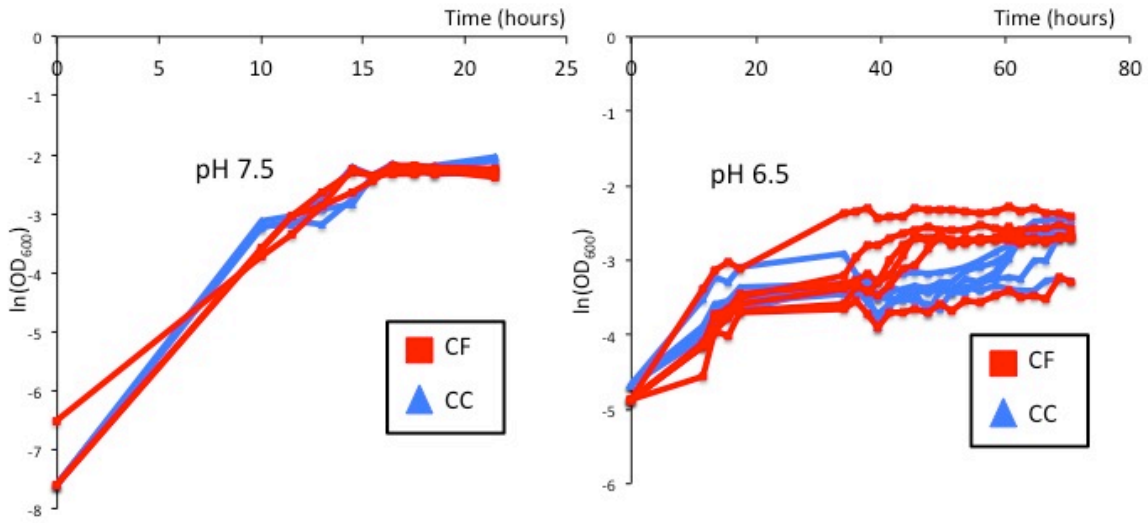

Supplementary Figure 3 Effect of pH on growth. We grew completely-consuming cells (lines CC) or nitrite (NO_2^-) cross-feeding cells (lines CF) at pH 7.5 (left panel) or pH 6.5 (right panel) with 10 mM of nitrate (NO_3^-) under anaerobic conditions. We measured the OD_{600} values over time. The data are plotted for n = 3 (pH 7.5) or n = 6 (pH 6.5) independent replicates.

Supplementary Tables

Supplementary Table 1 Bacterial strains and plasmids used for this study

Strain or plasmid	Relevant characteristics	Reference or source
***P. stutzeri* strain**		
A1501	wild-type strain	8
A1601	A1501 with Δ*comA*; defective in natural transformation	This study
A1602	A1501 with Δ*comA* and Δ*narG*; defective in natural transformation and nitrate reduction	This study
A1603	A1501 with Δ*comA* and Δ*nirS*; defective in natural transformation and nitrite reduction	This study
***E. coli* strain**		
DH5α/λpir	Used for replication of pAW19 derivatives; λ*pir*80*dlacZ*Δ*M15* Δ(*lacZYA-argG*)*U169 recA1 hsdr17 deoR thi-1 supE44 gyrA96 relA*	3
BW20767	Used for conjugative transfer of pAW19 derivatives; RP4-2-Tc::Mu-1 Kan::Tn*7* integrant *leu-63*::IS*10 recA1 zbf-5 creB510 hsdR17 endA1 thi uidA* (ΔMluI)::*pir*$^{+}$	1
Plasmid		
pAW19	*sacB*-containing conditionally replicative delivery plasmid; Ap^{R}, Km^{R}	1
pAW19-Δ*narG*	pAW19 with Δ*narG*; Ap^{R}, Km^{R}	This study
pAW19-Δ*nirS*	pAW19 with Δ*nirS*; Ap^{R}, Km^{R}	This study
pAW19-Δ*comA*	pAW19 with Δ*comA*; Ap^{R}, Km^{R}	This study

Supplementary Table 2 Oligonucelotide PCR primers used for cloning the *narG*, *nirS*, or *comA* gene deletions into the pAW19 plasmid

Gene deletion	Sequence amplified	Genome position	[a]Primer sequence (5'-3')	Restriction site
Δ*narG*	Upstream of *narG*	997369-998328	GGCGGCACTAGTGCGCTGGAAGTCAGCAC	SpeI
			GGCGGCGCGGCCGCCGTTTTCTCTCCTCACTCCG	NotI
	Downstream of *narG*	1002088-1003087	GGCGGCGCGGCCGCGGAATAAGGCCATGAAGATTCG	NotI
			GGCGGCGAGCTCTATACCGGCGACTTCTGCG	SacI
Δ*nirS*	Upstream of *nirS*	3817992-3818991	GGCGGCACTAGTGTGGGCTCGAGCTTCTGT	SpeI
			GGCGGCGCGGCCGCTCCGCCCGAGGATTG	NotI
	Downstream of *nirS*	3820675-3821669	GGCGGCGCGGCCGCCCTTCTCTCCTATGGGAGCG	NotI
			GGCGGCGAGCTCCCAGATCGTGCTGCTCCA	SacI
Δ*comA*	Upstream of *comA*	2855757-2856686	GGCGGCACTAGTTTGCCATTGAGCGAATAATTG	SpeI
			GGCGGCGCGGCCGCGAACGGCGGCCGTC	NotI
	Downstream of *comA*	2858913-2859912	GGCGGCGCGGCCGCTTTCAGTCTCCAGAAATCCTTTCC	NotI
			GGCGGCGAGCTCGACACTGGGGGCGACG	SacI

[a]Red: leader sequence for restriction digestion. Blue: restriction sequence. Black: target-specific sequence.

Supplementary references

1. Almeida JS, Júlio SM, Reis MA, Carrondo MJ. (1995a). Nitrite inhibition of denitrification by *Pseudomonas fluorescens*. *Biotechnol Bioeng* **46**: 194-201.
2. Almeida JS, Reis MA, Carrondo MJ. (1995b). Competition between nitrate and nitrite reduction in denitrification by *Pseudomonas fluorescens*. *Biotechnol Bioeng* **46**: 476-84.
3. Bryan BA, Jeter RM, Carlson CA. (1985). Inability of *Pseudomonas stutzeri* denitrification mutants with the phenotype of *Pseudomonas aeruginosa* to grow in nitrous oxide. *Appl Environ Microbiol* **50**: 1301-1303.
4. Metcalf WW, Jiang W, Daniels LL, Kim SK, Haldimann A, Wanner BL. (1996). Conditionally replicative and conjugative plasmids carrying lacZ alpha for cloning, mutagenesis, and allele replacement in bacteria. *Plasmid* **35**: 1-13.
5. Miller VL, Mekalanos JJ. (1988). A novel suicide vector and its use in construction of insertion mutations: osmoregulation of outer membrane proteins and virulence determinants in *Vibrio cholerae* requires toxR. *J Bacteriol* **170**: 2575-2583.
6. White AK, Metcalf WW. (2004). Two C-P lyase operons in *Pseudomonas stutzeri* and their roles in the oxidation of phosphonates, phosphite, and hypophosphite. *J Bacteriol* **186**: 4730-4739.
7. Wang JH, Baltzis BC, Lewandowski GA. (1995). Fundamental denitrification kinetic studies with *Pseudomonas denitrificans. Biotechnol Bioeng* **47**: 26-41.
8. Yan Y, Yang J, Dou Y, Chen M, Ping S, Peng J, *et al.* (2008). Nitrogen fixation island and rhizosphere competence traits in the genome of root-associated *Pseudomonas stutzeri* A1501. *Proc Natl Acad Sci USA* **105**: 7564-7569.